The Heart Surgery Forum #2005-1103
9 (5), 2006 [Epub June 2006]
doi:10.1532/HSF98.20051103 Online address: http://cardenjennings.metapress.com/link.asp?id=112496

Evaluation of Ascending Aortic Atherosclerosis with 16-Multidetector Computed Tomography Is Useful before Total Endoscopic Coronary Bypass Surgery

Gudrun Maria Feuchtner, MD,[1] Thomas Schachner, MD,[2] Nikolaos Bonaros, MD,[2] Alexander Smekal, MD,[1] Ammar Mallouhi, MD,[1] Guy J. Friedrich, MD,[3] Martin Deutschmann,[4] Guenther Laufer, MD,[2] Dieter zur Nedden, MD,[1] Johannes Bonatti, MD[2]

Departments of [1]Radiology II, [2]Cardiac Surgery, and [3]Cardiology, Innsbruck Medical University, Innsbruck; [4]Siemens Medical Solutions, Vienna, Austria

ABSTRACT

Background. The purpose of this study was to investigate the assessment of ascending aortic atherosclerosis with 16-multidetector computed tomography (16-MDCT) angiography prior to total endoscopic coronary artery bypass (TECAB) surgery.

Methods. Forty-five patients were examined with electrocardiogram-gated, 16-MDCT angiography. The presence of atherosclerosis at the ascending aorta was graduated as severe (>50% of circumference) or as mild (<50% of circumference). Ascending aortic plaque composition was evaluated based on CT densities expressed as Hounsfield units (HU). TECABs using the Da Vinci telemanipulator were performed either on the arrested heart (n = 39) with an intra-aortic cardiopulmonary bypass (CPB) perfusion device or on the beating heart (n = 6) in patients with severe atherosclerosis.

Results. The presence of mild atherosclerosis at the ascending aorta (11/39) was associated with intra-aortic CPB perfusion device–related difficulties such as intra-aortic balloon migration (BM) or balloon rupture (*P* = .007) in arrested heart TECABs. The CT density of atherosclerotic plaque in patients with BM was mean 58 HU ± 51 standard deviation (SD), suggesting noncalcifying plaque. In patients without BM, CT density of plaque was mean 526 HU ± 306 SD corresponding to calcifying plaque (*P* < .001). Balloon rupture occurred in 2 patients who had calcifying plaque at the ascending aorta.

Conclusion. Evaluation of ascending aortic atherosclerosis with 16-MDCT angiography is useful prior to TECAB surgery. Even mild atherosclerosis of the ascending aorta is associated with intraoperative difficulties regarding the remote-access perfusion system that is used for arrested heart TECAB surgery.

Received August 15, 2005; received in revised form April 21, 2006; accepted May 30, 2006.

Address correspondence and reprint requests to: Gudrun M. Feuchtner, MD, Department of Radiology II, Innsbruck Medical University, Anichstr. 35 A-6020, Innsbruck, Austria; 0043-512-504-81898; fax: 0043-512-504-24029 (e-mail: Gudrun.Feuchtner@uibk.ac.at).

INTRODUCTION

Totally endoscopic coronary artery bypass grafting (TECAB) represents a technique that allows surgical coronary revascularization without opening the chest. These operations have become feasible with the use of robotic systems such as the Da Vinci telemanipulator (Intuitive Surgical, Sunnyvale, CA, USA). TECABs may be performed either on the arrested heart (AH-TECAB) or on the beating heart (BH-TECAB) In AH-TECAB procedures, systemic circulation is maintained with an intra-aortic cardiopulmonary bypass (CPB) perfusion device that is topped with a balloon placed into the ascending aorta [Schachner 2004]. However, atherosclerosis of the ascending aorta may have adverse effects on the intra-aortic balloon.

Sixteen-multidetector computed tomography (16-MDCT) provides an emerging cardiovascular imaging modality. 16-MDCT is highly accurate for the detection of significant coronary artery stenosis [Hoffmann 2004; Küttner 2004; Hoffmann 2005; Mollet 2005] and has shown promising results in the assessment of coronary bypass graft patency [Nieman 2003; Schlosser 2004] (Figure 1). Myocardial bridging of the left anterior descending coronary artery (LAD) can be displayed well with 16-MDCT, which has already been shown to be useful prior to TECAB surgery to choose an appropriate anastomotic site [Herzog 2003]. Also, 16-MDCT allows reliable aorto-iliac angiography [Catalano 2004] and evaluation of atherosclerotic vessel wall affection and atherosclerotic plaque composition, noncalcifying plaque can be distinguished from calcifying plaque based on CT densities [Achenbach 2004; Leber 2004; Mollet 2005] in coronary arteries.

The aim of this study was to evaluate whether assessment of ascending aortic atherosclerosis is useful before TECAB surgery and whether the presence of ascending aortic atherosclerosis was correlated with intraoperative difficulties.

METHODS

Study Population

Forty-five patients (33 male, 12 female; mean age, 51 years; Table 1) who underwent TECAB surgery were examined

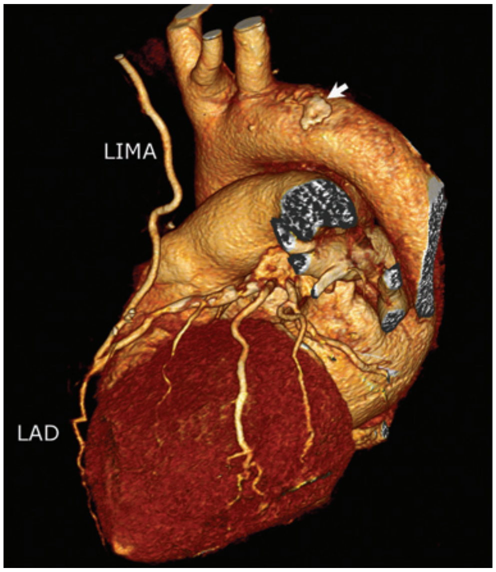

Figure 1. The postoperative computed tomography scan of a patient 1 week after arrested heart total endoscopic coronary artery bypass surgery. The left internal mammary artery (LIMA)/left anterior descending artery (LAD) bypass was found patent. A calcifying plaque at the aortic arch (white arrow) is shown by applying a volume-rendering technique.

between January 2002 and June 2005 within one week prior to surgical intervention. Patient exclusion criteria were contraindications against iodine contrast agent (eg, renal dysfunction, known allergy) and severe cardiac arrhythmia. Patients with an ascending aortic diameter >3.8 cm or severe atherosclerosis of the ascending aorta (>50% of the circumference) underwent BH-TECAB (n = 6); the remaining underwent AH-TECAB (n = 39). The Institutional Review Board approved the study. Written informed consent was obtained from all patients.

Operative Technique

TECABs were single left internal mammary artery (LIMA)-to-LAD using the Da Vinci telemanipulation system either on the BH or on the AH. In AH-TECABs, CPB was conducted using the ESTECH remote-access perfusion system (ESTECH, San Ramon, CA, USA) via cannulation of the left femoral artery. A 23, 25, or 27 F venous return cannula was placed into the left femoral vein. After balloon endo-occlusion, cardioplegia was performed with the St. Thomas solution. The anastomosis was sutured completely endoscopically as previously described [Schachner 2004].

Table 1. Patient Characteristics

Mean age	51
Male/female	33/12
Body mass index	26.6 ± 2.7
Arterial hypertension, n (%)	33 (73.3)
Peripheral arterial occlusive disease, n (%)	2 (4.4)
Cerebrovascular event, n (%)	1 (2.2)
Previous myocardial infarction, n (%)	12 (26.7)
Hypercholesterinemia, n (%)	32 (68.9)
Nicotineabusus, n (%)	21 (46.7)
Diabetes, n (%)	4 (8.9)

MDCT Examination Technique

All examinations were performed using a 16-MDCT scanner (Sensation 16; Siemens Medical Systems, Forchheim, Germany). Collimation was 16 × 0.75 mm; table translation speed, 6.7 mm/s; gantry rotation time, 0.42 seconds; tube current, 400 to 500 mAs; tube voltage 120 kV, and the effective radiation dose ranged between 4 and 10 mSv [Flohr 2002]. A bolus of 100 mL iodine contrast agent (Iodixanol, Visipaque 320; Amersham Health, Buckinghamshire, UK) was injected intravenously into an antecubital vein at a flow rate of 3 to 4 mL/s using a power injector (Ulrich Medizintechnik, Ulm, Germany). Scan delay was calculated by measuring CT attenuation values at the ascending aorta utilizing dedicated software (DynEva; Siemens) after the injection of a 20 mL test bolus of contrast agent. The time point of the highest CT attenuation was taken as the scan delay. Alternatively, a fixed scan delay of 20 seconds was used. Scanning was performed during a single-inspiratory breath hold of 20 to 28 seconds. A beta-blocker was injected intravenously (1-5 mg metoprololtartrate, Beloc; Schering-Plough, Kenilworth, NJ, USA) before the examination if the heart rate was greater than 75 bpm. Images were reconstructed with a smooth convolution kernel (B 10 f) or a medium smooth convolution kernel (B 30 f) at an increment of 0.6, 1-mm effective slice thickness, image matrix 512 × 512, FOV 130 to 190 mm, and by using retrospective electrocardiogram (ECG)-gating at mid-to-end diastole (60%-80% of RR interval). Images were then transferred to a dedicated off-line computed workstation (Leonardo; Siemens) and reconstructed using multiplanar reformation and a volume-rendering technique. Atherosclerosis of the ascending aorta was graded as mild if less than 50% of the circumference and as severe if more than 50% of the circumference was involved. Additionally, according to the echocardiographic criteria of Amarenco et al [1994], atherosclerosis was classified based on the ascending aortic wall thickness as: mild <1 mm, moderate 1 to 3.9 mm, and severe ≥4 mm. Atherosclerotic plaque morphology was determined by measuring CT densities within a region of interest. Several regions of interest were located at each ascending aortic plaque, and the mean value was calculated (lesion-based analysis). Also, any measurable atherosclerotic spot was considered a region of interest.

Statistical Analysis

Statistical analysis was performed with SSPS software (V8.0; SPSS, Chicago, IL, USA). The difference in Hounsfield units (HU) between patients with and without intra-aortic balloon migration (BM) was tested using independent samples and the *t* test. The correlation between remote-access perfusion system–related intraoperative complications and atherosclerosis of the ascending aorta was determined with chi-square test. A 2-tailed probability value <.05 was considered statistically significant.

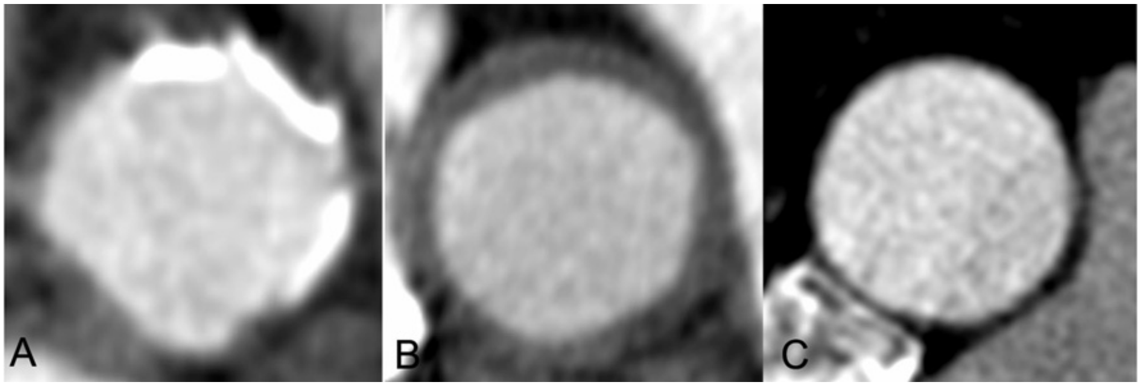

Figure 2. Preoperative computed tomography scan of the ascending aorta showing different atherosclerotic plaque types. A, Hyperdense, calcifying plaque (white). Intra-aortic balloon rupture occurred in this patient. B, Hypodense, noncalcifying plaque (dark) surrounding the complete ascending aortic lumen in a "rim-like" manner. C, There are no signs of atherosclerosis; note that the ascending aortic lumen is sharply delineated and smooth.

RESULTS

Mild atherosclerosis of the ascending aorta based on CT criteria (circumferential involvement) was noted in 11 of the 39 patients who underwent AH-TECAB. In 9 of the 11 patients with atherosclerosis, remote-access perfusion system–related complications such as intra-aortic BM or balloon rupture were noted (P = .007, chi-square). According to the echocardiographic criteria of Amarenco et al [1994], the aortic wall thickness in patients who underwent AH-TECAB was an average of 0.14 cm ± 0.03 standard deviation (SD) (range, 0.09-0.20 cm), corresponding to mild to moderate atheroslerosis. In patients in whom BH-TECAB was performed, atherosclerosis was moderate to severe (mean aortic wall thickness, 0.29 cm ± 0.11 SD; range, 0.19-0.41 cm). Ascending aortic risk factors [Schachner 2004] and patient characteristics are shown in Table 1.

On an atherosclerotic lesion-based analysis, mean CT density of atherosclerotic plaque (n = 15) in patients with BM was 58 HU ± 51 SD (range, 14-229 HU; Figure 3). In contrast, CT density of atherosclerotic plaque (n = 6) in patients without BM was mean 526 HU ± 306 SD (range, 63-851 HU). The difference between the groups was statistically significant (P < .001, t test; Figure 3). On an overall atherosclerotic-spots analysis (any atherosclerotic spots that were appropriate to measure: n = 45 spots in patients with BM versus n = 18 spots in patients without BM), the difference between the groups was significant as well (P < .001, t test). Intra-aortic balloon rupture was noted in 2 patients, both had calcifying plaque (Figure 2A) at the ascending aorta.

An aberrant right subclavian artery (Figure 4) was found in 2 patients; difficulties in intra-aortic balloon positioning by echocardiography were noted in one of those patients. Subsequently, the guide wire had to be monitored with x-ray to achieve a correct position of the balloon.

Myocardial bridging of the LAD (Figure 5) could be identified in 5 patients. Various intraoperative complications or technical difficulties were noted in 4 of the 5 patients (Table 2). None of these complications were significantly correlated with myocardial bridging. One patient had a right coronary artery myocardial bridging (Figure 5A).

DISCUSSION

This study shows that the evaluation of ascending aortic atherosclerosis with 16-MDCT is useful before TECAB surgery. The presence of mild ascending aortic atherosclerosis was associated with intraoperative difficulties regarding the remote-access perfusion system in AH-TECABs.

In particular, our data suggest that the presence of noncalcifying plaque (mean CT density, 58 HU) is correlated with intra-aortic BM. This may be explained by a lower static stiffness of noncalcifying plaque, which has already been shown with intravascular elastography [Lee 1992; de Korte 2000] in coronary arteries. In contrast, calcifying plaque was found in 2 patients in whom intra-aortic balloon rupture (n = 2) was noted. The balloon membrane in those 2 cases might have been too thin to tolerate the mechanical stress between the balloon and the calcifying spots.

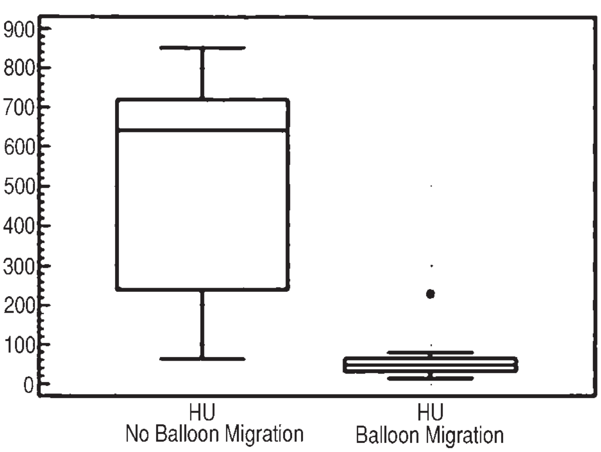

Figure 3. Box-and-whisker plot illustrates the difference in computed tomography (CT) densities of atherosclerotic plaques of the ascending aorta in patients with and without balloon migration (P < .001). Patients in whom intra-aortic balloon migration was noted had significantly lower plaque CT densities corresponding to noncalcifying plaque compared with patients without balloon migration. CT densities are expressed in Hounsfield units (HU) and are displayed on the y-axis.

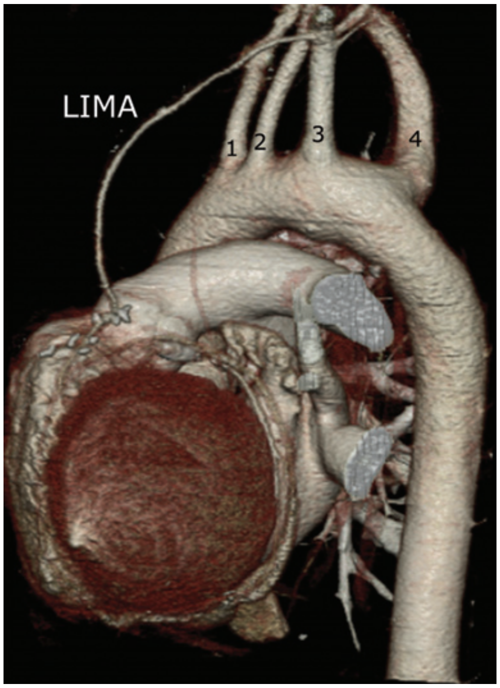

Figure 4. An aberrant right subclavian artery (4) may have a remarkable size, which may lead to difficulties in positioning the intra-aortic balloon with echocardiography because the guide wire may deviate. The number 1 indicates the right carotid artery; 2, left common carotid artery; 3, left subclavian artery. Postoperative 16-multidetector computed tomography scan was performed to assess left internal mammary artery (LIMA) graft patency. The image is 3-dimensionally displayed by applying a volume-rendering technique.

Table 2. Myocardial Bridging

Patient	Age	Intraoperative Complications or Modifications
1	38	Diagonal branch taken instead of left anterior descending coronary artery for revascularization
2	49	Diagonal branch taken instead of left anterior descending coronary artery; bleeding from right ventricular wall and conversion to sternotomy
3	53	Stenosis of anastomosis; revision and conversion to sternotomy
4	54	Bleeding from anastomotic heel requiring intraoperative elective dilatation
5	61	No intraoperative complications or modifications were noted

16-MDCT provides high spatial (0.5 × 0.5 × 0.6 mm^3) resolution and a temporal resolution of >105 ms [Flohr 2003], which has clearly improved plaque imaging. 16-MDCT allows a differentiation between noncalcifying ("soft") plaque and calcifying plaque [Achenbach 2004; Leber 2004; Mollet 2005] based on the visibility of hypodense plaque or hyperdense plaque components (Figure 2) and based on CT density measurement. For example, this has been investigated in a comparative study with intracoronary ultrasonography: noncalcifying, lipid-rich coronary plaque had a CT density of 49 HU and calcifying plaque had 391 HU [Leber 2004]. Additionally, advanced 16-MDCT technology offers retrospective ECG-gating, which allows motion artefact–free imaging of the ascending aorta [Roos 2002] and a display of aortic arch anomalies such as an aberrant right subclavian artery (Figure 4). An aberrant right subclavian artery is the most common aortic arch malformation with a prevalence of 0.4% to 2% [Soler 1998]. Note that aberrant right subclavian arteries may have a remarkable vessel size and may mislead the guide wire.

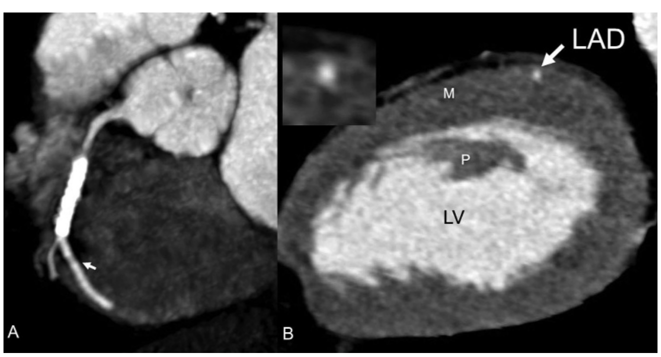

Figure 5. A, Myocardial bridging of the right coronary artery (RCA) shortly after a coronary stent by applying a maximum-intensity projection technique. The white arrow denotes the entrance of the RCA into the myocardium. B, The left anterior descending artery (LAD) clearly intramyocardially in another patient. Short axis view of the left ventricle. M indicates myocardium; LV, left ventricle; P, papillary muscle.

Furthermore, myocardial bridging of the LAD can be visualized well with 16-MDCT (Figure 5), which clearly had an influence on the selection of the anastomotic site [Herzog 2003]. In our series of investigations, we report a variety of intraoperative modifications and complications (Table 2) that might be partially related to myocardial bridging; for example, the presence of a myocardial bridging may lead to the decision to choose the take-off of a diagonal branch rather than the LAD. Some of those intraoperative complications might be explained by a more technically difficult suturing of the anastomosis. However, we found no statistically significant correlation of any intraoperative complication with myocardial bridging.

CONCLUSION

ECG-gated 16-MDCT angiography is useful in the assessment of the extent and composition of ascending aortic atherosclerosis prior to TECAB surgery. In patients with severe atherosclerosis, TECAB surgery should be performed on the beating heart. In AH-TECAB surgical procedures, even mild ascending aortic atherosclerosis was associated with intraoperative difficulties related to the intra-aortic CBP perfusion device. Intra-aortic BM was associated with noncalcifying plaque and calcifying plaque may cause balloon rupture. Advanced 16-MDCT image post-processing techniques are helpful for the detection of mild ascending aortic atherosclerosis.

REFERENCES

Achenbach S, Moselewski F, Ropers D, et al. 2004. Detection of calcified and noncalcified coronary atherosclerotic plaque by contrast-enhanced, submillimeter multidetector spiral computed tomography: a segment-based comparison with intravascular ultrasound. Circulation 109:14-7.

Amarenco P, Cohen A, Tzourio C, et al. 1994. Atherosclerotic disease of the aortic arch and the risk of ischemic stroke. N Engl J Med 331:1474-9.

Catalano C, Fraioli F, Laghi A. 2004. Infrarenal aortic and lower-extremity arterial disease: diagnostic performance of multi-detector row CT angiography. Radiology 231:555-63.

de Korte CL, Pasterkamp G, van der Steen AF, et al. 2000. Characterization of plaque components with intravascular ultrasound elastography in human femoral and coronary arteries in vitro. Circulation 102:617-23.

Flohr T, Bruder H, Stierstorfer K, et al. 2002. New technical developments in multislice CT, part 2. Sub-millimeter 16-slice scanning and increased gantry rotation speed for cardiac imaging. Rofo Fortschr Geb Roentgenstr 174:1023-7.

Herzog C, Dogan S, Diebold T, et al. 2003. Multi-detector row CT versus coronary angiography: preoperative evaluation before totally endoscopic coronary artery bypass grafting. Radiology 229:200-8.

Hoffmann U, Moselewski F, Cury RC, et al. 2004. Predictive value of 16-slice multidetector spiral computed tomography to detect significant obstructive coronary artery disease in patients at high risk for coronary artery disease: patient-versus segment-based analysis. Circulation 110:2638-43.

Hoffmann M, Shi H, Schmitz B, et al. 2005. Non-invasive coronary angiography with multislice computed tomography. JAMA 293:2471-8.

Kuettner A, Kopp A, Schroeder S, et al. 2004. Diagnostic accuracy of multidetector computed angiography in patients with angiographically proven coronary artery disease. J Am Coll Cardiol 43:831-9.

Leber AW, Knez A, Becker A, et al. 2004. Accuracy of multidetector spiral computed tomography in identifying and differentiating the composition of coronary atherosclerotic plaques: a comparative study with intracoronary ultrasound. J Am Coll Cardiol 43:1241-7.

Lee RT, Richardson SG, Loree HM, et al. 1992. Prediction of mechanical forces of human atherosclerotic plaque by high-frequency intravascular ultrasound imaging. A vitro study. Arterioscler Thromb 12:1-5.

Mollet NR, Cademartiri F, Krestin GP, et al. 2005. Improved diagnostic accuracy with 16-row multi-slice computed tomography coronary angiography. J Am Coll Cardiol 45:128-32.

Mollet NR, Cademartiri F, Nieman K, et al. 2005. Noninvasive assessment of coronary plaque burden using multislice computed tomography. Am J Cardiol 95:1165-9.

Nieman K, Pattynama PMT, Rensing BJ, et al. 2003. Evaluation of patients after coronary artery bypass surgery: angiographic assessment of grafts and coronary arteries. Radiology 229:749-56.

Roos JE, Willmann JK, Weishaupt D, et al. 2002. Thoracic aorta: motion artifact reduction with retrospective and prospective electrocardiography-assisted multi-detector row CT. Radiology 222:271-7.

Schachner T, Bonaros N, Laufer G, et al. 2004. The ESTECH remote access perfusion cannula in minimally invasive cardiac surgery. Heart Surg Forum 7:E632-5.

Schachner T, Nagele G, Kacani A, Laufer G, Bonatti J. 2004. Factors associated with presence of ascending aortic atherosclerosis in CABG patients. Ann Thorac Surg 78:2028-32.

Schlosser T, Konorza T, Hunold P, et al. 2004. Noninvasive visualization of coronary artery bypass grafts using 16-detector row computed tomography. J Am Coll Cardiol 44:1224-9.

Soler R, Rodriguez E, Requejo I, et al. 1998. Magnetic resonance imaging of congenital abnormalities of the thoracic aorta. Eur Radiol 8:540-6.